Point defect reactions at surfaces and in bulk metals

C. P. Flynn
Physics Department and Materials Research Laboratory, University of Illinois at Urbana-Champaign, Urbana, Illinois 61801, USA
(Received 1 September 2004; published 28 February 2005)

This paper describes the time evolution of reacting defect assemblies both in bulk metals and on their surfaces. Three areas are treated. The first describes the linear response of reacting assemblies to perturbing fields such as irradiation or temperature change. Alternative long wavelength limits identified here concern: (i) independent diffusion of vacancy- and interstitial-type defects to sinks; and (ii) joint diffusion of defects down a chemical potential gradient, with a separate branch of solutions associated with recombination. The second topic concerns definitions of the chemical potential μ^* and temperature T^* associated with the defect system itself, as distinct from the properties of the embedding lattice. The utility of these quantities is illustrated by examples including those pertaining to rapid temperature change. μ^* and T differ from the lattice values μ, T, to an extent that determines possible energy and particle transfer in such processes as nucleation of new sinks and precipitation from the defect assembly. The role of these quantities in relaxation modes is clarified. Finally, an appendix discusses an approximate model of defect behavior in the bulk, and a speculative discussion of defect behavior on surfaces, both positing homologous properties of the defect systems in metals, when scaled to the melting temperature T_m. These characteristics of a standard metal and a standard close-packed metal surface are employed in the text to identify and contrast typical behaviors of the bulk and surface defect systems of metals. Universal properties that follow from these models are discussed in a second appendix.

DOI: 10.1103/PhysRevB.71.085422 PACS number(s): 68.35.Dv, 66.30.Lw, 61.72.−y, 68.35.Fx

I. INTRODUCTION

It is a well-established fact that the kinetics of atomic processes, both in the bulk of crystals[1–5] and on surfaces,[6–8] are mediated by thermal defects. These defects take the form of vacant sites and of added atoms that occur in the bulk as interstitials and on surfaces as adatoms. In each case the two species are antidefects. Thermal defects achieve equilibrium populations by creation and annihilation at such sinks as surface steps and bulk dislocations. They also react as antidefects that form by spontaneous fluctuations of the perfect lattice, and also mutually annihilate by random encounters; once more, this is the case for both surface and bulk systems. Energy is conserved through transfer to vibrational and electronic processes. When the defect systems are driven strongly, for example, by irradiation,[9,10] and even in thermal equilibrium, notably on surfaces above half the melting temperature T_m, defect concentrations can become sufficiently large that reactions dominate the defect life cycle. Then transport and kinetics take place through processes characteristic of the reacting defect assembly.

The present paper treats this problem with particular emphasis on metallic crystals, and on phenomena that occur when a defect assembly remains close to its thermal equilibrium configuration. The thermodynamic variables pertinent to atomic transfer between defect systems and lattice sites are also considered. Related processes specifically induced by irradiation are treated, but an exploration of their main consequences is deferred to a later work.[11]

Although much is known about thermal defects in the bulk of metallic crystals,[1–5,9,10,12] for surface defects the state of understanding is much less advanced.[6–8,13–16] In the bulk, vacancies dominate transport near equilibrium; both the formation and motion free energies of vacancies and interstitial atoms have been surveyed for a range of pure metals.[12] The properties turn out to be surprisingly systematic when scaled by melting temperature T_m.[17,18,2,9] In Appendix A this effective scaling is employed to create a standard metal whose defect properties are representative of metals in general, from which specific cases may differ to a greater or lesser but not large extent. Throughout the paper this model is employed to assess the results of calculations for reacting bulk defect assemblies.

Similar modeling of systematic trends has been suggested[19] but not yet justified for surface defects, for which information about mass diffusion comes largely from studies of step edge fluctuations[20–23] and scratch smoothing.[24,25] Indeed, various surface orientations of the same crystal must surely behave differently. Appendix A nevertheless identifies a standard close-packed metal surface whose properties generally mimic the known behavior of surface species. This is employed in the text to track typical properties expected for interacting assemblies on close-packed metal surfaces, that remain still to be charted by experiment. A point of particular interest is that the modeling affirms a compelling distinction between surface and bulk behavior, which originates in the large surface defect populations associated with the relatively small creation free energies of surface thermal defects. While the experimental facts about surfaces remain insufficiently documented at present, these differences appear large enough to remain pertinent as more information accumulates.

The properties of reacting thermal defects in crystals have been studied for many decades.[26,2,5] Early seminal ideas developed for insulators[26,4] where charged defects couple in predictable ways. Later work included metals, where interactions are short-ranged, but nevertheless still cause nonlinear transport behavior where high densities of vacancies lead to defect reactions.[27–30,10] On the other hand, most information about interstitial atoms in metals derives either from

computer simulations or experiments on weakly irradiated bulk crystals at low temperatures.[10,12] Treatises, textbooks, and reviews cited above summarize the available information.

For surface processes the factual base of defect parameters is much less well developed. For example, the temperature-dependent concentration of thermal defects is accurately known scarcely for a single instance,[31] and for most metal surfaces, even the dominant thermal defect has not been identified unambiguously. Careful experiments have nevertheless determined the activation energies for hopping motion of adatoms in a number of cases,[32] mostly for low temperatures $\sim T_m/5$. Despite this paucity of factual information, the reactions of defects on surfaces can still be charted prospectively in terms of formation and motion parameters that remain to be verified. For the present, these results offer model predictions of surface properties for comparison with bulk behavior, by inspection of the standard close-packed surface and the standard metal, as described above.

In Sec. II below, the equations needed to describe the evolution of defect assemblies are sufficiently nonspecific as to apply equally to surface and bulk defects. The reactions of their formation and annihilation are formulated generally, in Sec. II A, with surface and bulk processes following a common format. In Sec. II B the partial differential equations are solved for conditions close to equilibrium. The character of the relaxation modes so determined is investigated in Sec. II C. In the absence of inhomogeneous driving terms, and for reaction controlled conditions, there are two sets of modes that pertain, respectively, in the long wavelength limit, first to recombination and second to long-range diffusion of both defect species down the chemical potential gradient to sinks. Section II D then employs the standard metal, and standard close-packed surface parameters, to survey the regimes into which bulk and surface phenomena fall as the temperature is varied from T_m to zero. Clear distinctions between surface and bulk behavior arise from this comparison.

In Sec. III the thermodynamic of the reacting assembly is discussed in terms of a newly defined local temperature T^* and chemical potential μ^* of the reacting assembly. This clarifies questions of heat and particle transfer among parts of a system and between two distinct assemblies, for example, surface and bulk. The space and time dependence of defect formation after temperature change is treated as a pertinent example. The models of standard behavior for bulk and surface defects are deferred to Appendix A. Finally, Appendix B presents illustrative cases in which the standard models predict universal behavior for defect systems in metals.

For completeness we remark here that the results of the present paper provide the basis for further investigations in which defect systems, including defect interactions, are driven by external fields, for example, by irradiation. Thus the work presented here provides the response of reacting assemblies to a particle flux, which causes radiation damage and defect flow in the bulk, and such important phenomena as beam-accelerated kinetics and enhanced growth processes on surfaces. Detailed results for such processes, however, are deferred to a separate publication.[11]

II. THERMAL DEFECTS IN THE BULK AND ON SURFACES OF METALS

This section formulates equations to describe reactions that create and annihilate point defects in the bulk of crystals and on crystal surfaces. We treat materials formed from a single chemical species, although this limitation is imposed for clarity and simplicity rather than for fundamental reasons. In the bulk of such materials, thermal point defects comprise either an extra atom inserted into the lattice, as an interstitial, or else a missing atom, leaving a vacant site, or vacancy. These defects are mobile and interact also with crystalline surfaces, to which they typically bind with a release of free energy. Vacancies are incorporated into the surface layer as advacancies, while interstitials find their most stable surface configuration at specific sites exterior to surfaces terraces as adatoms. The ad-defect properties must depend on the particular orientation and state of the surface.

The equations that determine defect evolution recognize three factors. First, external driving forces can create defects either independently or as antidefect pairs. Second, both in the bulk and on surfaces, two antidefects can react and mutually annihilate when they meet; in thermal equilibrium, the inverse process of spontaneous creation by lattice fluctuations occurs in the perfect lattice at an equal rate, to produce detailed balance. Third, all point defects undergo separate annihilation and creation also, at special sites known as sinks. It is convenient to emphasize sinks that are translationally invariant, such that multiple defect processes cause at most a spatial displacement of the sink, and its free energy remains unchanged. Then the sink provides a locus at which the defect chemical potential is zero. If necessary it is possible to treat the departure of real sinks from this ideal behavior. Examples of sinks are step edges at which a surface terrace terminates, that act as sinks for both species of addefects, and also for bulk defects, while a variety of structures such as edge dislocations, interior voids, and surfaces also act as sinks for bulk defects.

A. Evolution of reacting defect assemblies

Antidefect populations change with time owing to reactions, to diffusion, and to the action of such perturbing processes as irradiation, evaporation, etc. Several terms are readily assembled to obtain partial differential equations that describe the consequent time evolution. The purpose here is to determine the evolutions of the distributions $c_1(\mathbf{r},t), c_2(\mathbf{r},t)$ of reacting defects under conditions that promote inhomogeneity, time dependence, or both.

Reaction and diffusion both depend on the mobilities of the defects. Specifically, the rates at which the two species meet and mutually annihilate in the lattice depends on the rate at which they explore new sites, and hence on their diffusion coefficients D_1, D_2. The latter determine defect flow by $\mathbf{J}_i = \Omega_i^{-1} D_i \nabla c_i$, and the hopping frequency by $w_i = 2dD_i/l_i^2 N_i$, along each of N_i nearest neighbor jump paths with length l_i. Here d is the dimensionality, namely, 2 for surface and 3 for bulk processes. The volume Ω_i per site in the first of these equations converts the occupancy c_i into a number of defects per unit volume, C_i. For the surface pro-

cess the surface area A per site enters the result instead.

In terms of these contributions the defect loss rates by reaction at $\mathbf{r},t$ are

$$\begin{aligned}\dot{c}_1(\mathbf{r},t) &= \dot{c}_2(\mathbf{r},t)\\ &= -\frac{\lambda_1 D_1 + \lambda_2 D_2}{a^2} c_1(\mathbf{r},t)c_2(\mathbf{r},t)\\ &= -K_{12}c_1(\mathbf{r},t)c_2(\mathbf{r},t),\end{aligned} \tag{1}$$

Here, a is the lattice parameter and $\lambda_i=\alpha_i a^2/l_i^2$, with α_i a constant that depends on the mutual separation at which antidefect pairs annihilate, such that typically $\lambda\sim 50$ for the bulk and perhaps half that for surfaces (our notation follows that of Lee *et al.*[33]). Note in addition that detailed balance among microscopic processes is achieved only if defects are created spontaneously in the lattice at a rate

$$\dot{c}_1(\mathbf{r},t) = \dot{c}_2(\mathbf{r},t) = K_{12}\overline{c_1}\,\overline{c_2}, \tag{2}$$

with $\overline{c_1},\overline{c_2}$ the *equilibrium* concentrations, independent of $\mathbf{r},t$. The net rates from reactions are thus

$$\dot{c}_1(\mathbf{r},t) = \dot{c}_2(\mathbf{r},t) = -K_{12}[c_1(\mathbf{r},t)c_2(\mathbf{r},t) - \overline{c_1}\,\overline{c_2}]. \tag{3}$$

Defects also flow through and from the location $\mathbf{r}$ by diffusion. These processes conserve particles other than at fixed sinks, where annihilation and creation take place. If sinks are translationally invariant, defect processes at most displace the sink slowly to a configuration of equal energy, and such sinks accordingly establish the local chemical potential for the defects at its equilibrium value μ for the lattice at ambient temperature T. It follows from the diffusion equation that the defect loss rates from diffusion satisfy

$$\begin{aligned}\dot{c}_1(\mathbf{r},t) &= D_1\nabla^2[c_1(\mathbf{r},\mathbf{t}) - \overline{c_1}],\\ \dot{c}_2(\mathbf{r},t) &= D_2\nabla^2[c_2(\mathbf{r},\mathbf{t}) - \overline{c_2}].\end{aligned} \tag{4}$$

These diffusion equations are to be solved subject to the condition that $c_i-\overline{c_i}=0$ at the boundary sites of fixed sinks, where $\overline{c_i}$ is established by the equilibrium chemical potential μ of the lattice at temperature T.

B. Formulation for the linear regime

In addition to reaction and diffusion, many interesting phenomena occur while defects are simultaneously created or destroyed by externally impresses processes, such as irradiation. These may possibly be spatially inhomogeneous and time dependent. Representing the resulting creation rates by

$$\dot{c}_1 = K_1(\mathbf{r},t); \quad \dot{c}_2 = K_2(\mathbf{r},t) \tag{5}$$

for the two species, we obtain complete equations for the time evolution of c_1 and c_2:

$$\begin{aligned}\dot{c}_1 - D_1\nabla^2(c_1-\overline{c_1}) - K_{12}(\overline{c_1}\,\overline{c_2} - c_1c_2) &= K_1(\mathbf{r},t);\\ \dot{c}_2 - D_2\nabla^2(c_2-\overline{c_2}) - K_{12}(\overline{c_1}\,\overline{c_2} - c_1c_2) &= K_2(\mathbf{r},t).\end{aligned} \tag{6}$$

These equations can, in principle, be solved for any specific example and the behavior of the defect populations thus determined.[34,35] The equations are, however, nonlinear, so that general solutions are not readily achieved. A variety of computational approaches have been described; a recent perspective is given by Doan and Martin.[35]

Here we focus on the general behavior of reacting defect systems close to equilibrium. An example in point might be the response of a surface defect population to the small perturbation caused by the Gibbs–Thompson potential of a curved step edge;[21] the response in turn determines the relaxation times characteristic of the step fluctuation spectrum. Close to equilibrium the response must become linear,[23] and a description of this type of linear regime is our primary goal.

The nonlinear systems are linearized by writing $c_1=\overline{c_1}+s_1; c_2=\overline{c_2}+s_2$. Then

$$\begin{aligned}\left[\frac{\partial}{\partial t} - D_1\nabla^2 + K_{12}\overline{c_2}\right]s_1 &= -K_{12}\overline{c_1}s_2 + K_1(\mathbf{r},t);\\ \left[\frac{\partial}{\partial t} - D_2\nabla^2 + K_{12}\overline{c_1}\right]s_2 &= -K_{12}\overline{c_2}s_1 + K_2(\mathbf{r},t).\end{aligned} \tag{7}$$

Nonlinear terms in c_1c_2 are thus eliminated, and the system of equations becomes linear in s_1,s_2. They are to be solved subject to the boundary condition $s_1,s_2=0$ at fixed sinks, where $c_i=\overline{c_i}$.

The solutions of Eqs. (7) in any particular case comprise solutions of the homogeneous equations obtained when $K_1,K_2=0$, supplemented by particular integrals that accommodate the terms in K_1 and K_2. The former are of interest here; the latter are treated as they arise in particular contexts. Representing by $[\,]_1$ and $[\,]_2$ the differential operators in braces on the left, we obtain for $K_1,K_2=0$ the equations

$$\begin{aligned}[\,]_1[\,]_2 s_2 &= -K_{12}\overline{c_2}[\,]_1 s_1 = K_{12}^2\overline{c_1}\,\overline{c_2}s_2;\\ [\,]_2[\,]_1 s_1 &= -K_{12}\overline{c_1}[\,]_2 s_2 = K_{12}^2\overline{c_1}\,\overline{c_2}s_1.\end{aligned} \tag{8}$$

Consequently both s_1 and s_2 are solutions of the homogeneous equation

$$\begin{aligned}&\left\{\left[\frac{\partial}{\partial t} - D_1\nabla^2 + K_{12}\overline{c_2}\right]\left[\frac{\partial}{\partial t} - D_2\nabla^2 + K_{12}\overline{c_1}\right]\right.\\ &\qquad\left. - K_{12}^2\overline{c_1}\,\overline{c_2}\right\}s(\mathbf{r},t)\\ &= 0.\end{aligned} \tag{9}$$

We seek solutions of the form

$$s(\mathbf{r},t) = s\exp(i\mathbf{q}\cdot\mathbf{r})\exp(-wt).$$

Equation ((9)) transforms to

$$\left\{\left[-w + q^2D_1 + K_{12}\overline{c_2}\right]\left[-w + q^2D_2 + K_{12}\overline{c_1}\right] - K_{12}^2\overline{c_1}\,\overline{c_2}\right\}s = 0, \tag{10}$$

or

$$w^2 - [K_{12}(\overline{c_1} + \overline{c_2}) + q^2(D_1 + D_2)]w + q^2(D_1\overline{c_1} + D_2\overline{c_2})K_{12} + q^4 D_1 D_2 = 0. \tag{11}$$

This quadratic equation has solutions

$$w = b \pm (b^2 - c)^{1/2}, \tag{12}$$

in which

$$b = [K_{12}(\overline{c_1} + \overline{c_2}) + q^2(D_1 + D_2)]/2;$$
$$c = q^2(D_1\overline{c_1} + D_2\overline{c_2})K_{12} + q^4 D_1 D_2. \tag{13}$$

These give the required eigenvalues, $w(\mathbf{q})$, of the system of Eq. (9). They afford plane wave solutions of the homogeneous relaxation problem for reacting defect systems near equilibrium. The question of what boundary conditions the plane wave eigenvalues are chosen to satisfy is discussed below in Sec. III C.

C. Character of the relaxation modes

The modes derived above show how the departure $s(\mathbf{r},t)$ of defect populations from equilibrium relaxes back toward zero as time passes. It does so generally as a sum of eigenfunctions, each decaying exponentially:

$$s(\mathbf{r},t) = \sum_{\mathbf{q}} \alpha_{\mathbf{q}} s_{\mathbf{q}}(\mathbf{r}) \exp[-w(\mathbf{q})t]. \tag{14}$$

The eigenfunctions $s(\mathbf{r})$ are not generally plane waves but, rather, combinations of plane waves that satisfy the boundary conditions $s=0$ at fixed sinks. In this connection note that the eigenvalues w derived above depend only on $q=|\mathbf{q}|$. Consequently the $s_{\mathbf{q}}(\mathbf{r})$ are appropriate sums over plane waves having the same q and a common decay rate; thus

$$s_{qj}(\mathbf{r}) = \sum_{|\mathbf{q}|=q} \beta_{\mathbf{q}j} \exp(i\mathbf{q}\cdot\mathbf{r}); \tag{15}$$

$$s(\mathbf{r},t) = \sum_{qj} \alpha_{qj} s_{qj}(\mathbf{r}) \exp[-w(q)t]. \tag{16}$$

Here, the $s_{qj}(\mathbf{r})$ may be selected to form an orthonormal set.

The two defect species have concentrations defined by similar expansions but with different constants α_{qj} in a ratio fixed by the eigenvalue $w(q)$, as evaluated here. For $K_1 = K_2 = 0$, Eqs. (6) read

$$[-w(q) + q^2 D_1 + K_{12}\overline{c_2}]s_1 = -K_{12}\overline{c_1}s_2;$$
$$[-w(q) + q^2 D_2 + K_{12}\overline{c_1}]s_2 = -K_{12}\overline{c_2}s_1; \tag{17}$$

whence for the two modes the two species have relative amplitude given by

$$s^{\pm} = (s_2/s_1)^{\pm} = \frac{a_1 - a_2}{2b_1}\left[1 \pm \left(1 + \frac{4b_1 b_2}{(a_1 - a_2)^2}\right)^{1/2}\right], \tag{18}$$

in which

$$a_1 = q^2 D_1 + K_{12}\overline{c_2}; \quad b_1 = -K_{12}\overline{c_1};$$
$$a_2 = q^2 D_2 + K_{12}\overline{c_1}; \quad b_2 = -K_{12}\overline{c_2}. \tag{19}$$

Useful, in addition, are the exact identities:

$$s^+ s^- = -\overline{c_2}/\overline{c_1};$$
$$s^+ + s^- = -[q^2(D_1 - D_2) + K_{12}(\overline{c_1} - \overline{c_2})]/K_{12}\overline{c_1}. \tag{20}$$

These equations define the ratios of the decay mode amplitudes of the two species for the two modes (i.e., $\pm$) that are characteristic of any particular eigenmode q,j. Some illustrative examples follow.

1. Diffusion dominated decay

The values of q required by the diffusion equation are determined by the geometry of the sinks. It may happen (and is commonly the case in bulk examples at high temperatures) that the diffusive loss greatly exceeds the recombination, and the recovery is therefore dominated by defect diffusion to the sinks, with $a_1, a_2 \gg b_1, b_2$. Then the above equations are best rearranged to give

$$w_{\pm} = \frac{1}{2}(a_1 + a_2) \pm \frac{1}{2}\left[(a_1 - a_2)^2 + 4b_1 b_2\right]^{1/2};$$
$$s^{\pm} = \frac{1}{2b_1}\left\{(a_1 - a_2) \mp \left[(a_1 - a_2)^2 + 4b_1 b_2\right]^{1/2}\right\}. \tag{21}$$

The first now gives

$$w_+ = a_1 \approx q^2 D_1; \quad w_- = a_2 \approx q^2 D_2; \tag{22}$$

and the ratios of the defect amplitudes are

$$(s_2/s_1)^- \approx (a_1 - a_2)/b_1 = -[q^2(D_1 - D_2) + K_{12}(\overline{c_2} - \overline{c_1})]/K_{12}\overline{c_1};$$
$$(s_1/s_2)^+ \approx (a_2 - a_1)/b_2 = [q^2(D_1 - D_2) + K_{12}(\overline{c_2} - \overline{c_1})]/K_{12}\overline{c_2}. \tag{23}$$

Both ratios are large (note that the second is inverted), provided that $D_1 \neq D_2$, so that the two modes largely comprise separate diffusion of defects 1 and 2 to their fixed sinks. In each case the corrections to this limiting behavior concern ratios of recombination to diffusion, as expected. The dispersion curves for this case are shown as functions of q in Fig. 1(a) for the example $D_1/D_2 = 3$. The flow corresponding to such modes is represented below by the arrows near the equilibrium point in Sec. III B, Fig. 6(a).

2. Equal diffusion

When $D_1 = D_2 = D$ the exact results are obtained precisely as above:

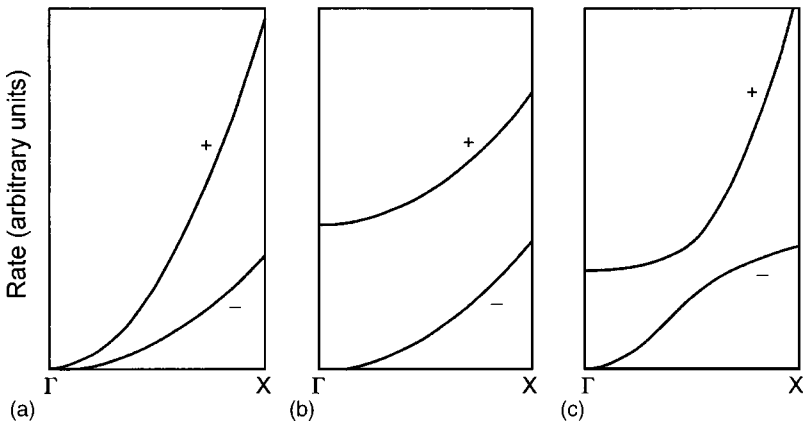

FIG. 1. Dispersion relations for relaxation in several cases. (a) Independent diffusion of the two species to sinks arises when recombination is negligible compared to diffusion. (b) Equal diffusion and recombination rates of two species leads to one branch purely diffusion and one (upper) mixed recombination and diffusion. (c) When diffusion and recombination compete in midzone the dispersions exhibit an avoided crossing. At the zone center the two branches are pure diffusion and pure recombination (see text).

$$w_{\pm} = q^2 D + \frac{1}{2}K_{12}(\overline{c_1} + \overline{c_2}) \pm \frac{1}{2}K_{12}(\overline{c_1} + \overline{c_2});$$
$$s^{\pm} = \frac{\overline{c_1} - \overline{c_2}}{2\overline{c_1}}\left[1 \pm \frac{\overline{c_1} + \overline{c_2}}{\overline{c_1} - \overline{c_2}}\right], \tag{24}$$

so that

$$w_{+} = q^2 D + K_{12}(\overline{c_1} + \overline{c_2}); \quad (s_2/s_1)^{+} = 1;$$
$$w_{-} = q^2 D; \quad (s_2/s_1)^{-} = -\overline{c_2}/\overline{c_1}. \tag{25}$$

These dispersion relationships are shown in Fig. 1(b). Evidently the + mode comprises recombination (which causes equal decays of the two species) with diffusion (for $q \neq 0$) while the − mode decays entirely by diffusion. In this regard note that the − mode corresponds to equal but opposite *fractional* departures from equilibrium for the two species. As such it is consistent with the two species responding to a common but inhomogeneous chemical potential in the lattice (see also below and Sec. III).

3. One loss term dominant

When, as must normally occur, one loss rate from diffusion or recombination greatly exceeds the other three terms, the equations are best rearranged so the roots can be expanded to provide immediate approximations to the eigenvalues and the amplitude ratios. Thus

$$w_{\pm} = \frac{1}{2}(a_1 + a_2)\left\{1 \pm \left[1 + \frac{4(b_1 b_2 - a_1 a_2)}{(a_1 + a_2)^2}\right]^{1/2}\right\};$$
$$s^{\pm} = \frac{1}{2b_1}\left\{(a_1 - a_2) \mp (a_1 + a_2)\left[1 + \frac{4(b_1 b_2 - a_1 a_2)}{(a_1 + a_2)^2}\right]^{1/2}\right\}. \tag{26}$$

With only one term large, and b_2 and b_1 also contained in a_1 and a_2, respectively, the ratio inside the root is small. By expansion one finds

$$w_{+} = \frac{q^2(D_1\overline{c_2} + D_2\overline{c_1}) + K_{12}(\overline{c_1} + \overline{c_2})^2}{(\overline{c_1} + \overline{c_2})};$$
$$(s_2/s_1)^{+} \approx 1 - \frac{q^2(D_1 - D_2)}{K_{12}(\overline{c_1} + \overline{c_2})};$$
$$w_{-} = \frac{q^2(D_1\overline{c_1} + D_2\overline{c_2})K_{12} + q^4 D_1 D_2}{K_{12}(\overline{c_1} + \overline{c_2}) + q^2(D_1 + D_2)}; \tag{27}$$
$$(s_2/s_1)^{-} \approx -\overline{c_2}/\overline{c_1}\left(1 - \frac{q^2(D_1 - D_2)}{K_{12}(\overline{c_1} + \overline{c_2})}\right),$$

where the results for s are for small q. Both ± results warrant comment. The + mode has the decay rate of whichever process is dominant. As $q \to 0$ it becomes the recombination term $K_{12}(\overline{c_1} + \overline{c_2})$ alone, and accordingly the ratio of defect densities becomes unity. On the other hand, as $q \to 0$, the − mode identifies an effective diffusion coefficient,

$$D_{\text{eff}} = \frac{(D_1\overline{c_1} + D_2\overline{c_2})}{(\overline{c_1} + \overline{c_2})}, \tag{28}$$

comprising the mass diffusion coefficient (less correlation factors) divided by the net defect concentration. This is the diffusion coefficient with which the reacting defect assembly responds to a gradient of defect chemical potential, according to the Nernst–Einstein equation $J = -[(c_1 + c_2)D_{\text{eff}}/\Omega k_B T]\nabla\mu$. It is analogous to the "thermal equilibrium" D_{eff} obtained[2,28] for reacting vacancies that maintain local equilibrium. For the − mode as $q \to 0$, the ratio of defect amplitudes becomes $s_2/s_1 = -\overline{c_2}/\overline{c_1}$, which is consistent with the defect fluxes driven by a common chemical potential. The relaxation modes have the dispersion relationships shown in Fig. 1(c), and for $q \to 0$ are indicated by arrows near the equilibrium point in Sec. III B, Fig. 6(b).

The condition that a single rate term is largest may be valid only over some range of q as, for example, when the q dependence of the diffusion terms overtakes recombination terms with increasing q. In the exact dispersion curves shown in Fig. 1(c), one diffusion coefficient is a factor of 10 larger than the other. It crosses the larger of the recombination rates halfway to the Brillouin zone boundary, with the smaller recombination rate fixed an order of magnitude smaller. As evident in Fig. 1(c), the exact dispersion curves

exhibit an avoided crossing where the rates of the faster diffusion process and faster recombination process become equal.

D. Relaxation of surface and bulk defects

We now compare and contrast reactions among thermal defects on close-packed surfaces with those in the bulk of metals. One purpose is to clarify and illustrate the results of the preceding sections by application to typical materials. In particular, the complexity of surface diffusion, as defined by the standard close-packed surface, becomes clearly apparent. Also, the equilibrium properties recognized here establish a base for a future discussion of the reactions that take place when these systems are driven by particle irradiation.[11]

The four parameters that enter into the reaction kinetics, according to Eqs. (7), are q^2D_1 and $K_{12}c_2$ for added atom defects and q^2D_2 and $K_{12}c_1$ for vacancies. To show generally how these behave, Fig. 2(a) for bulk defects compares D_1 with $R_1=K_{12}c_2/q^2$ (broken lines), and D_2 with $R_2=K_{12}c_1/q^2$ (solid lines). The choice made here for $q\sim n\pi/L$ is the smallest eigenvalue ($n=1$) for a region of length $L=10$ μm, a relatively large sink spacing, selected here to enhance bulk reactions relative to defect diffusion to fixed sinks. Even so, D_2 and R_2 for the dominant vacancy defects become equal only just below T_m. Thus, for the standard metal, the majority defects form mostly at sinks, except in the range $\sim T_m$ to $0.8T_m$, where pairs in the bulk mainly form by spontaneous fluctuation. It is of some interest that even this limited range of reaction-controlled conditions could not be identified before the recent discovery that interstitial formation entropies are so large[36,37] (see Appendix A).

A similar calculation for surface species is shown in Fig. 2(b). The eigenvalue q is chosen for sinks separated by $L=0.1$ μm, appropriate for step edges on a surface miscut by 0.1°. The large diffusion rates of the surface defects more than compensate for the factor 10^2 in sink spacing between the surface and bulk systems, chosen for this comparison. The estimated crossings of R and D for surface species occur near $0.3T_m$ and $0.4T_m$ for (majority) adatoms and (minority) advacancies, respectively. Evidently surface antidefects are controlled by pair reactions over most of the temperature range below T_m.

We conclude that significant distinctions separate bulk and surface kinetics. Spontaneous creation of pairs on the terraces dominates surface defect processes on low miscut surfaces at temperatures above $\sim T_m/3$ whereas, in the bulk, the majority defects become reaction controlled only just below T_m.

Also owing to the large concentration of surface defects, defect multiples occur on surfaces at high temperatures to the degree that it may possibly become impractical to describe the total defect population by building blocks of defect multiplets. The adatom concentration [Eq. ((A7))] $c_1\sim 3\exp(-4.5T_m/T)$ reaches 3.3×10^{-2} at T_m. The density of adatom *pairs* at T_m, given an estimated pair binding energy one-third of the adatom formation energy, is then $3c_1^2\exp(-1.5T_m/T)\sim 1.5\times10^{-2}$; thus about as many adatoms are bound in pairs as exist singly on the surface. Because defect formation energies were obtained in Appendix A by assigning to them most of the activation energy for mass diffusion, as actually *observed* at $T>T_m/2$, it is hard to see how actual defect densities could be much smaller than those described here. Given the many possible triplet configurations, and that some may be strongly bound, the total occupation of the surface by adatoms at T_m is generally large, and may be poorly defined for the parameters of a standard close-packed surface. Certainly, in the bulk, defect concentrations larger than about 1% [e.g., for AgI (Ref. 37)] cause the relevant sublattice to become *liquidlike*.

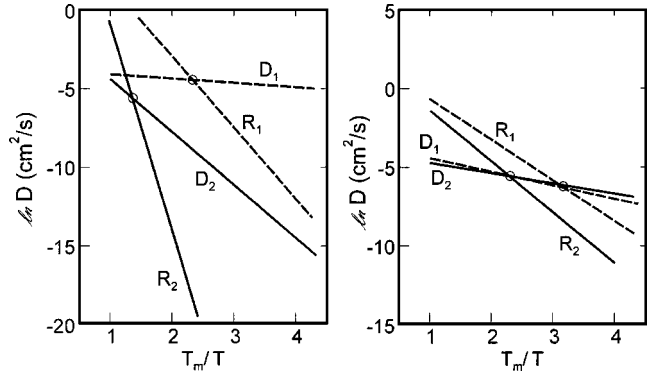

FIG. 2. Relative diffusion and recombination for bulk defects (a) and surface defects (b) evaluated for standard metal, with 10 μm bulk sink spacing and 100 nm surface sink spacing. For each defect, D is the diffusion coefficient and R measures the relative rate of recombination for $q=1$ (the longest wavelength mode). For the bulk, majority defects (vacancies) only just achieve reaction limited kinetics at T_m, whereas surfaces are reaction controlled above $T_m/3$ even with the smaller sink spacing.

Experimental observation of liquidlike behavior in the surface layer has been reported for some metal surfaces.[38,39] In regard to diffusion, it is known that even large, compact islands remain mobile on close-packed surfaces,[40] so a complete treatment must certainly include complexes and reactions. For less smooth surfaces, with smaller formation energies, the defect densities are still larger, and the contribution of complex processes to defect flow must accordingly be still greater.

These conclusions have significant consequences. Surface diffusion is a critical process that facilitates epitaxial growth, surface fluctuations and smoothing, and other technically important phenomena. The present discussion suggests, for $T>T_m/3$, that measurements of surface mass diffusion (e.g., by step fluctuation spectroscopy), and all processes determined by mass diffusion, are likely to involve an effective diffusion coefficient for the reacting assembly, as in Eq. (28), rather than activated linear diffusion of one independent defect species. At the highest temperatures, and for less smooth surfaces, it is likely that sizable defect clusters contribute to mass flow, and a more careful and complete theory of mass flow is therefore needed.

III. TEMPERATURE AND CHEMICAL POTENTIAL IN REACTING ASSEMBLIES

Our concern here lies with reacting defects in nonequilibrium assemblies; the local values of c_1, c_2 then may generally

differ from the thermal equilibrium values $\overline{c_1}, \overline{c_2}$. In this connection it is useful to recall,[2] for the added-atom defect in the dilute limit ($c \ll 1$), that the *equilibrium* densities of thermal defects are

$$\overline{c_1} = \exp - f_1/k_BT = \exp[-(F_1 - \mu)/k_BT]; \tag{29a}$$

similarly,

$$\overline{c_2} = \exp - f_2/k_BT = \exp[-(F_2 + \mu)/k_BT] \tag{29b}$$

for vacancy type defect. In these equations T and μ are the equilibrium temperature and chemical potential of the lattice, F_1 is the work required to place an atom from infinity into the site occupied by the extra atom, and F_2 is the work needed to remove an atom to infinity from a site of the perfect lattice, in order to create a vacancy (the number of sites per lattice site for added atom defects can be incorporated into F_1). f_1 and f_2 are thus the free energies of defect formation, which have energy and entropy components quantified explicitly in Appendix A. Finally μ is the average work (a negative quantity) required to add one atom from infinity to a typical bound site of the solid, exemplified as the binding energy at a kink site at a surface step. This latter definition provides a sink that remains unchanged by the process, other than by a translation that has no consequence for the free energies (i.e., the kink site has the average energy of the atoms of the crystal).

When c_1 and c_2 differ locally from their equilibrium values, we can regard the temperature and chemical potential of the defect system as taking effective values T^* and μ^* defined by

$$\begin{aligned} c_1 &= \exp[-(F_1 - \mu^*)/k_BT^*]; \\ c_2 &= \exp[-(F_2 + \mu^*)/k_BT^*], \end{aligned} \tag{30}$$

in which c_1, c_2 replace the equilibrium values $\overline{c_1}, \overline{c_2}$. Thus T^* and μ^* are the lattice temperature and chemical potential with which these defect densities would be in equilibrium. Then from Eqs. (30):

$$T^* = T\frac{\ln \overline{c_1}\overline{c_2}}{\ln c_1 c_2}; \tag{31a}$$

$$\begin{aligned} \mu^* - \mu &= \frac{1}{2}k_B[T^* \ln(c_1/c_2) - T\ln(\overline{c_1}/\overline{c_2})] \\ &= \frac{1}{2}k_BT\left[\frac{\ln \overline{c_1}\overline{c_2}\,\ln(c_1/c_2)}{\ln c_1 c_2} - \ln(\overline{c_1}/\overline{c_2})\right], \end{aligned} \tag{31b}$$

after elimination of T^*. Note that T^* and μ^* represent the temperature and chemical potential *of the defect system itself*; they determine, for example, energy and particle flow between parts of the system, and between the defect system and the lattice. Of course, the values of T^*, μ^* may differ from the lattice values T, μ, whenever the defect system is driven by forces that affect the defect system independently, as in the cases of irradiation, rapid change of lattice temperature, or mechanical work.

As an illustration in what follows we consider first the way T^* and μ^* evolve with time as the lattice undergoes sudden changes of temperature. The relationship to the normal relaxation modes derived in Sec. II is then discussed for bulk and surface systems.

A. Pair generation remote from sinks after quenching

At equilibrium, the spontaneous annihilation, that occurs as antidefects encounter each other in the lattice by diffusion, is precisely compensated by the creation of antidefect pairs by spontaneous fluctuations of the perfect lattice. No local precursor structure is necessary for this latter process to operate. When temperature changes occur, the creation processes respond accordingly with changed rates appropriate to the new temperature. However, annihilation continues at a rate fixed by the existing defect site occupancies in Eq. (3), albeit with kinetics adjusted to the new temperature. A characteristic evolution of defect populations occurs by reaction, both on terraces and in the bulk, to a state of kinetic equilibrium determined by the new temperature. While all such processes may be modeled by computation, it turns out that an exact solution can be written down for the particular problem. This section summarizes the result and its consequences for the defect temperature and chemical potential.

We consider a lattice with uniform occupancies, c_1, c_2, of defects corresponding to equilibrium at the initial temperature, perturbed by a temperature change for which the equilibrium occupancies now become $\overline{c_1}, \overline{c_2}$. This problem can be solved exactly. In the absence of sinks, Eqs. (6) for the evolution both read

$$K_{12}^{-1}\dot{s} = \overline{c_1}\overline{c_2} - (c_1 + s)(c_2 + s), \tag{32}$$

in which $s(t)$ is the added occupancy for both species due to reactions at the new temperature. Our concern here is to find $s(t)$ and the consequent defect properties $T^*(t)$ and $\mu^*(t)$. Equation (32) may be integrated and a constant of integration selected to fit the initial conditions, yielding

$$s(t) = c\left[\frac{\varepsilon \coth(t/\tau) + 1}{\varepsilon + \coth(t/\tau)} - \varepsilon\right], \tag{33}$$

in which

$$\begin{aligned} c^2 &= \overline{c_1}\overline{c_2} + (c_1 - c_2)^2/4; \quad \tau^{-1} = cK_{12}; \\ \varepsilon &= (c_1 + c_2)/2c. \end{aligned} \tag{34}$$

Thus $s \to 0$ at $t=0$; and $s \to c(1-\varepsilon) = c - (c_1 + c_2)/2$ as $t \to \infty$, which gives $s \to (\overline{c_1}\overline{c_2})^{1/2}$ if $\overline{c_1}\overline{c_2} \gg c_1 c_2$, when the system is heated, and $s \to -c_1$ or $-c_2$, depending on the sign of the root, when the system is quenched, with $\overline{c_1}\overline{c_2} \ll c_1 c_2$.

The changes of the defect chemical potential μ^* caused by the evolution of the defect system are of special interest as they promote defect precipitation, creating new sinks, when μ^* departs sufficiently from the lattice chemical potential μ. μ^* is obtained from

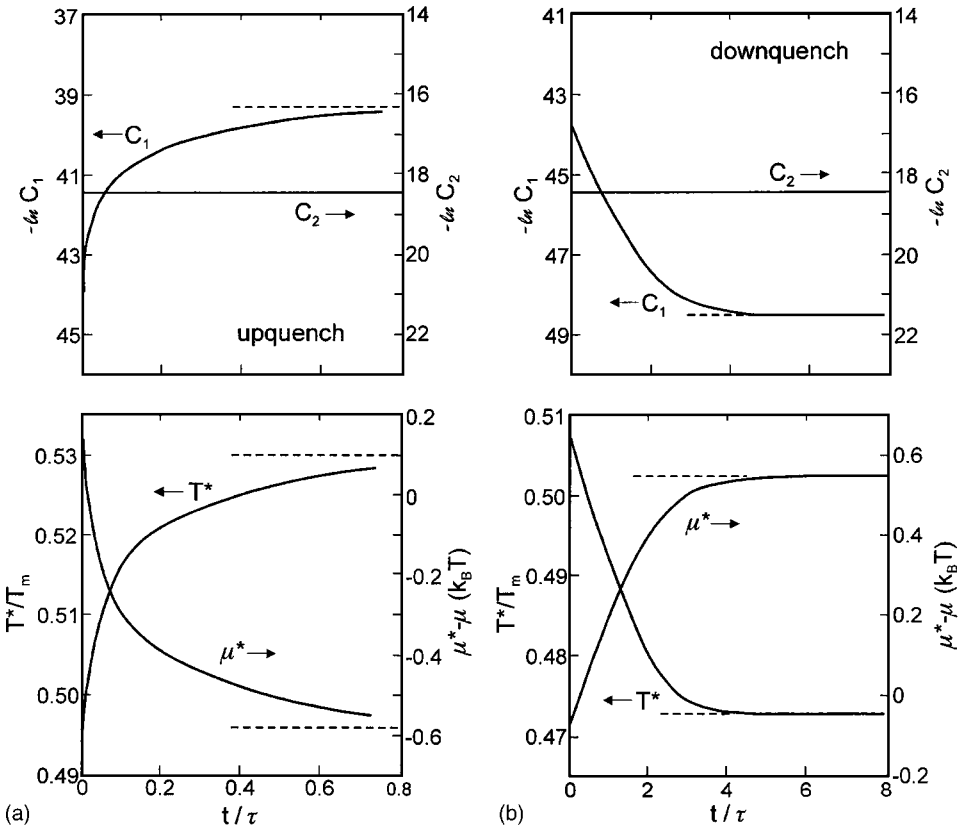

FIG. 3. Time evolution of bulk defect concentrations (top) for a standard metal that is instantly (a) upquenched and (b) downquenched from $T=0.5T_m$ to change the final equilibrium value of c_1c_2 by factors of $10^{\pm 2}$. The concurrent changes of T^* and $\mu^*-\mu$ are shown below. The latter exhibit instantaneous changes at $t=0$ due to the temperature dependence of F. Note that the small required changes of T still cause nonlinear response, readily visible from the differing timescales in (a) and (b).

$$\mu^* - \mu = \frac{1}{2}k_B[T^* \ln(c_1+s)/(c_2+s) - T\ln(\overline{c_1}/\overline{c_2})];$$

$$T^* = T\frac{\ln \overline{c_1}\overline{c_2}}{\ln(c_1+s)(c_2+s)}, \tag{35}$$

using

$$\frac{(c_1+s)}{(c_2+s)} = \frac{c_1[\coth(t/\tau)+\varepsilon]+c(1-\varepsilon^2)}{c_2[\coth(t/\tau)+\varepsilon]+c(1-\varepsilon^2)};$$

$$(c_1+s)(c_2+s) = \overline{c_1}\overline{c_2} - \frac{\overline{c_1}\overline{c_2}-c_1c_2}{[\cosh(t/\tau)+\varepsilon\sinh(t/\tau)]^2}. \tag{36}$$

In verifying these results, note that the first of Eqs. (36) clearly gives c_1/c_2 as $t\to 0$, and as $t\to\infty$ gives $[c_1+s(\infty)]/[c_2+s(\infty)]$ with $s(\infty)=c(1-\varepsilon)$, as required. The product in the second equation becomes c_1c_2 as $t\to 0$, and $\overline{c_1}\overline{c_2}$ as $t\to\infty$, again as is necessary.

Figure 3 shows the evolution of c_1, c_2, μ^*, and T^* for a standard metal initially at $T=0.5T_m$ for two cases in which the reacting defects pass toward a kinetic equilibrium after a sudden temperature change. In Fig. 3(a), $\overline{c_1}\overline{c_2}=10^2c_1c_2$, as a temperature rise $\Delta T/T\sim 0.03T_m$ *increases* the defect population, and in Fig. 3(b), $\overline{c_1}\overline{c_2}=10^{-2}c_1c_2$, when a quench of similar magnitude *decreases* the concentrations. c_2 hardly changes because the steady state is achieved by variations of c_1 by factors of $\sim 10^{\pm 2}$. Initially T^* jumps slightly in the opposite sense from the initial lattice temperature in both examples, and then changes smoothly to equilibrate at the new *lattice* temperature, with a response time $\sim cK_{12}^{-1}$. The initial jump arises from the dependence of F_1+F_2 on T in Eqs. (30) (i.e., the defect formation entropies). Note that the factors 10^2 in c_1, c_2, from even these small fractional temperature changes, place the response far outside the linear regime, so that the actual responses in (a) and (b) differ by an order of magnitude in duration.

After a similar initial small jump, the chemical potential μ^* of the defect system relaxes back through μ and departs progressively further as the reaction takes place. This behavior of μ^* can readily be understood from the fact that the relative proportions of the defects change as the defect populations evolve under the reaction constraint that additional defects of the two types form or annihilate in equal numbers. Temperature increase then creates a relative excess of the minority defect (for that temperature) while, after quenching, the majority species consumes the minority and results in a minority deficit. The defect chemical potential μ^* therefore departs from μ in the opposite sense for the two cases. A point of special interest is that the results shown in Fig. 3 are universal, applying to all metals, in the approximation of Appendix A; indeed, the decay times for different metals are identical function of T/T_m (see below and Appendix B).

The change of chemical potential caused by pair creation allows the lattice to access new channels for relaxation. When μ^* differs sufficiently from the lattice value μ, a system can lower its free energy by new channels when defects react to nucleate fresh sinks, such as dislocation loops in the bulk, or step edges on the surface; these serve as centers at which, for each species, the thermal excess defects may be annihilated and deficient species created, thereby restoring

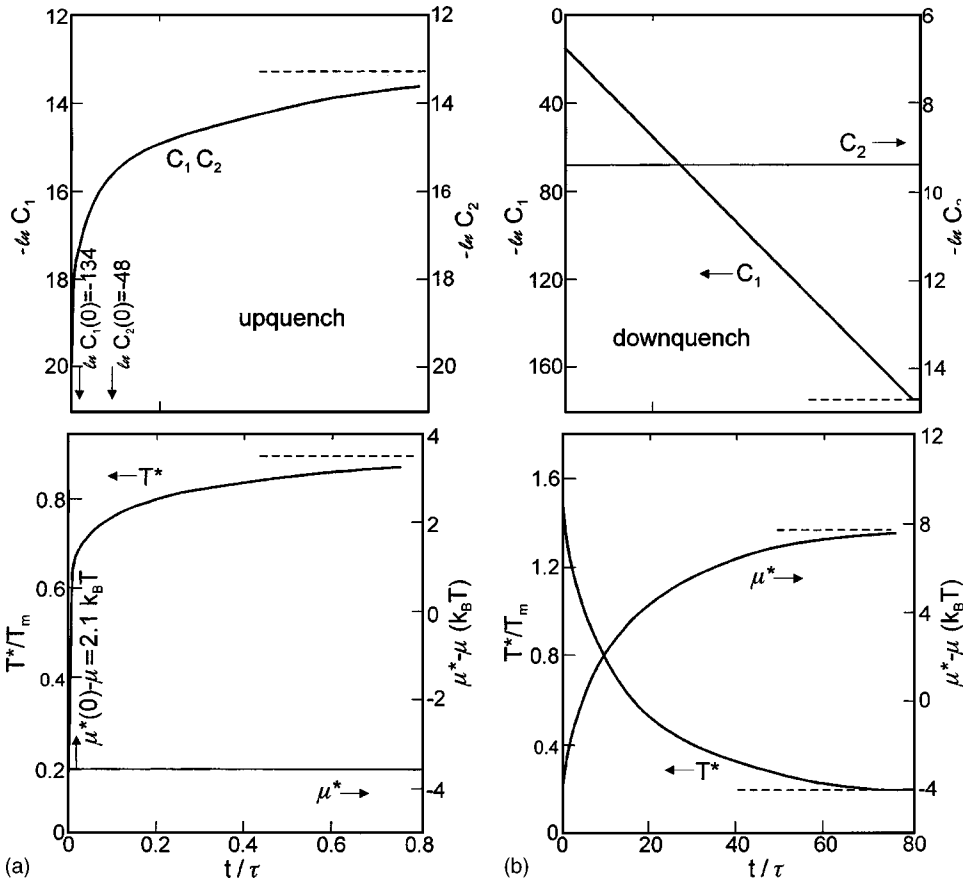

FIG. 4. Time evolution of bulk defect concentrations (top) for a standard metal that is (a) instantly upquenched from $0.2T_m$ to $0.9T_m$ and (b) downquenched from $0.9T_m$ to $0.2T_m$. The concurrent changes of T^* and $\mu^*-\mu$ are shown below. The latter exhibit instantaneous changes at $t=0$ due to the temperature dependence of F. On the upquench, c_1 and c_2 are equal from very short times because, after the temperature increase, the lattice creates equal excesses, and the chemical potential is thereby pinned (see text). Steady state after the downquench requires many multiples of the relaxation time τ because c_1 changes by so many orders of magnitude.

true equilibrium. Such nucleation events may require substantial chemical potentials which, for the small temperature changes examined in Fig. 3, are not available, with $|\mu^*-\mu|<0.1$ eV in typical cases. Much larger potentials are available for larger temperature changes. The following illustration is chosen to clarify the utility of the T^*,μ^* formulation.

Consider then the changes that occur when the bulk of a standard metal in equilibrium at $0.2T_m$ is suddenly heated to $0.9T_m$; and also the reverse process of quenching from $0.9T_m$ to $0.2T_m$ (the latter is typical of experiments to study vacancies in metals such as Au, with $0.2T_m$ near room temperature). The evolutions of c_1, c_2, T^*, and μ^* are shown in Fig. 4. On the up-quench [Fig. 4(a)] the final interstitial density exceeds the initial vacancy density, so both species are generated in the lattice and quickly achieve essentially equal concentrations. The initial defect population c_1,c_2, when first present at the final temperature, gives $\mu^*-\mu=-2.0k_BT_m$, which rises to $3.6k_BT_m$ as new defects then form to reach their steady (but nonequilibrium) state at $0.9T_m$. The increase favors excess interstitials and here represents the *maximum* increase, which makes the densities of the two species essentially equal (for which $\mu^*-\mu=(10-7.17T/T_m)k_BT_m$; this is the value, for example, when irradiation creates essentially equal excesses of the two antidefects). In the case of Fig. 4(b) for the down-quench to $0.2T_m$ from $0.9T_m$, the vacancies consume almost all the interstitials, and the density reduction by so many orders of magnitude takes correspondingly many multiples ($\sim$160) of the response time τ. In Fig. 4(b), the initial value at $0.2T_m$ is $\mu^*-\mu=3.2k_BT_m$, which then decreases to $-7.8k_BT_m$ at the steady state. For the example of Au metal this is over 1 eV, which is amply sufficient to influence nucleation of new sinks. The negative sign of the final μ^* indicates that vacancies have become more prevalent, at the expense of interstitials, which are suppressed by the large negative μ^* [cf. Eqs. (30)].

Note that precisely the same magnitude ($7.8k_BT_m$) can be obtained when, instead, the *interstitial* chemical potential is written, as is customary, $\Delta\mu_i=k_BT\ln c_1/\overline{c_1}=-7.8k_BT_m$, with c_1 the final defect occupation after reaction (in this case T and T^* are equal). The analogous result for vacancies is $\Delta\mu_v=k_BT\ln c_2/\overline{c_2}=+7.8k_BT_m$, with c_2 and $\overline{c_2}$ the equilibrium and final vacancy concentrations. These opposite results for $\Delta\mu_i$ and $\Delta\mu_v$ do show correctly that, at sinks where $\Delta\mu_i,\Delta\mu_v=0$, vacancy *annihilation* and interstitial formation are equally enhanced in the steady state defect configuration.

The distinction between the $\Delta\mu_i,\Delta\mu_v$ notation and the present T^*,μ^* formulation becomes clear from the values after the quench but *before* the reaction occurs. The results are $\Delta\mu_v=+7.8k_BT_m$ (unchanged, since the number of vacancies hardly changes in the reaction with interstitials) while $\Delta\mu_i=+11.7k_BT_m$. An inference from the (almost unchanged) majority (vacancy) population, and consequent $\Delta\mu_v$, that the tendency of the majority defect to precipitate remained unchanged through the reaction would, unfortunately, be in error. In fact, the balance of defect stability evolves from interstitial precipitation to vacancy precipitation as the defect reaction progresses at $0.2T_m$. Specifically, before the reaction, the force driving interstitial *annihilation* is even greater than the analogous force for vacancies, so that new lattice sites (e.g., interstitial loops) form rather than disappear. Note

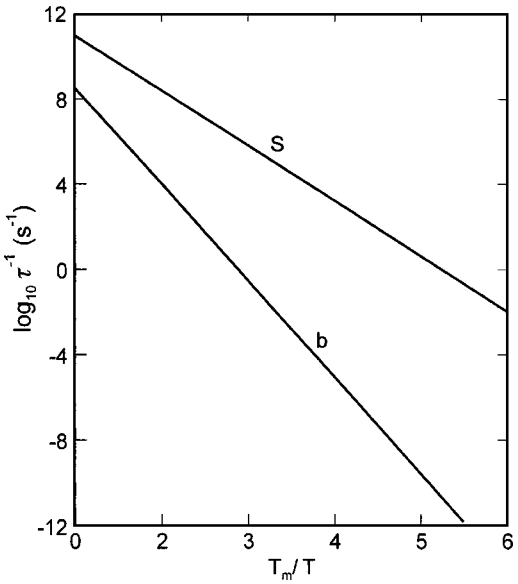

FIG. 5. Relaxation rates for surface (s) and bulk (b) defect systems for a standard metal, shown as functions of temperature. In this approximation, the τ^{-1} are universal functions of T/T_m.

that, in contrast, the actual switch during reaction from net interstitial to net vacancy precipitation is correctly monitored by the potential μ^* which changes from $2.1k_BT_m$, through zero, to $-7.8k_BT_m$, as the defects evolve to a steady state at $T=0.2T_m$. In short, the T^*,μ^* formulation fulfills its purpose of monitoring the *net* reactivity (chemical potential) of the *composite* defect system.

We can predict the bulk and surface relaxation times from small perturbations, for both bulk and surface processes, as functions of temperature. These are universal functions of T/T_m within the standard metal approximations. When $\overline{c_1},\overline{c_2}\approx c_1,c_2,c\rightarrow(c_1+c_2)/2$ in Eq. (34), so $\tau^{-1}\rightarrow K_{12}(c_1+c_2)/2$. For the bulk, $c_2\gg c_1$, and $D_1\gg D_2$, so that $\tau^{-1}\rightarrow\lambda c_2D_1/2a^2$. The result for the bulk shown in Fig. 5 is obtained with $\lambda=50, a=4\times10^{-8}$ cm, and the values of c_2D_1 given for a standard metal in Appendix A, so that the process is activated with an energy $10.5k_BT_m$. If, for surfaces, adatoms are both the more prevalent and the more mobile, then the result for surfaces is approximately $\tau^{-1}\rightarrow\lambda c_1D_1/2a^2$ in which the surface mass diffusion coefficient $c_1D_1\sim5\times10^{-4}\exp(-6T_m/T)$ cm^2/s. With $\lambda\sim25$ for the smaller surface atom coordination, the relaxation time in Fig. 5 corresponds to an activation energy of $6k_BT_m$. As seen in Fig. 5, the bulk and surface times at T_m are 30 ns and 10 ps, respectively, and the former remains the smaller at all temperatures. They pass through laboratory times ~1 s at about $0.4T_m$ and $0.2T_m$, respectively. Note that these are now decay times in linear response for small perturbations, in which equilibrium defects dominate the reaction. Of course, these results may need refining as data accumulate, and in any event will differ to some extent from one actual metal to the next.

Two further comments on the use of T^*,μ^* follow. First, upon quenching surface defects, the changes of chemical potential are much smaller than for the bulk because the formation energies are smaller; and also the equilibrium occupancies for the two antidefects are more comparable. Second, the use of these ideas, and the access the system acquires to new pathways for relaxation, is not restricted to temperature change, but instead is common to all pair creation phenomena including, for example, irradiation events which cause local modifications of chemical potential that nucleate new sinks such as interstitial loops in the bulk, and activate step edge flow on surfaces. A specific discussion of this nucleation and subsequent flow is deferred to a separate publication.

We note finally that both T^* and μ^* remain finite as $T\rightarrow0$ even when defects remain present. This may offer a basis for the discussion of simulations of defective driven systems[41] in which questions of free energy and phase change remain interesting at 0 K.[42]

B. Application to surface and bulk relaxation modes

Here we place the relaxation modes of bulk and surface defect systems, as described in Sec. II, in the context of the temperature T^* and chemical potential μ^* of the defect system, introduced in Sec. III. To interpret any particular case note that T^* is constant for fixed values of c_1c_2. The defect chemical potential μ^* is constant when $\ln c_1=\alpha\ln c_2$; then $\mu^*-\mu=(k_BT/2)[(1-\alpha)/(1+\alpha)]\ln\overline{c_1}\overline{c_2}-\ln(\overline{c_1}/\overline{c_2})$, with α a constant. On a graph with axes $\ln c_1$ and $\ln c_2$, constant μ^* appears as a straight line through $c_1=c_2=1$, both logarithms then being zero. Constant T^* occurs instead for straight lines of slope -1. The cases shown in Fig. 6 employ a modification of this scheme with coordinates $\ln(c_1/\overline{c_1}),\ln(c_2/\overline{c_2})$. With this choice, thermal equilibrium is shifted to the point (0,0), and the straight lines of constant μ^* now converge at the point $\ln c_1^{-1},\ln c_2^{-1}$.

These plots may be employed to display the different behaviors of reaction-controlled and independently diffusing defects. Figure 6(a) shows the example, typical of bulk defects at $T_m/2$, for which the standard metal (Appendix A) gives $\overline{c_1}\ll\overline{c_2}\sim10^{-8}$. Lines of constant T are shown, with a common slope, and lines of constant μ which converge to the point described above are labeled in units of $k_BT/2=k_BT_m/4$. In addition, a thick broken line shows for this case the changes near equilibrium (at the coordinate origin) caused by Frenkel pair formation or recombination.

Our interest centers on the relaxation modes revealed in the linear response formulation. As explained in Sec. II, the mode character depends on the separation of free sinks. For reasonable sink separations ~10 μm, and defect properties for $T_m/2$ given by the standard metal, the recombination turns out to have negligible effect. Then the two relaxation modes reduce to the independent modes in which the two defect species diffuse separately to the free sinks. Figure 1(a) shows dispersion relationships typical of this type of behavior. Small arrows near the equilibrium point (0,0) in Fig. 6(a) indicate the displacements of these normal modes from equilibrium.

The bulk behavior at $T_m/2$ documented above is contrasted in Fig. 6(b) with the typical case for defect relaxation on surfaces at $\sim T_m/2$ where concentrations $c_1,c_2,\sim10^{-4}$ are expected for a standard metal surface. For a separation ~0.1 μm between sinks, the recombination terms are now

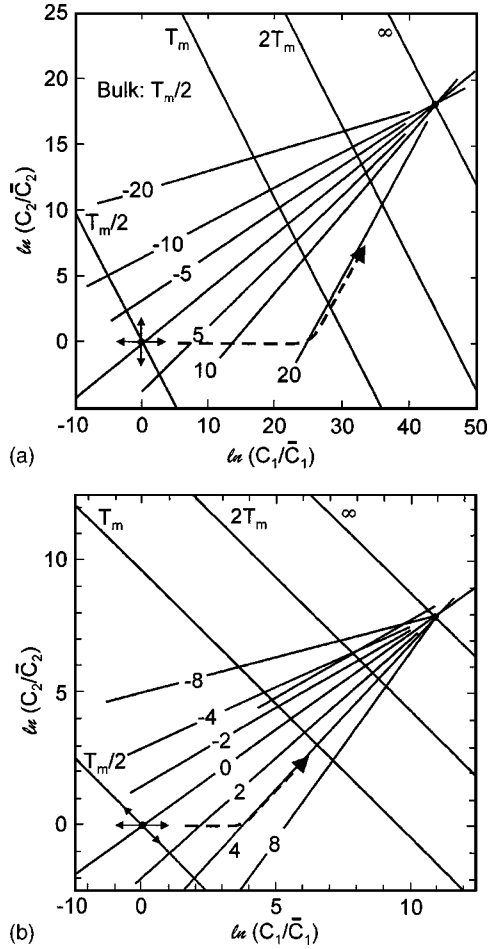

FIG. 6. T^* and μ^* shown as functions of c_1, c_2 at $T=T_m/2$ for the standard bulk metal (a) and the standard close-packed metal surface (b). Lines of constant T^* have a common slope, and lines of constant μ, marked in units of $k_BT/2$ converge to the point $\ln c_1^{-1}, \ln c_2^{-1}$. A heavy broken line indicates Frenkel pair formation near equilibrium, at (0,0). The orthogonal relaxation modes, calculated in Sec. II, and indicated by arrows at (0,0) in the figure, correspond to separate diffusion of the species to sinks in (a), and in (b) to Frenkel pair reactions and joint isothermal diffusion down a chemical potential gradient. The difference arises from typical defect concentrations relative to typical sink spacings for the two cases.

dominant, and the two relaxation modes for $q \to 0$ in Fig. 1(c) have $s_1=s_2$ and $s_1/s_2=-\overline{c_1}/\overline{c_2}$ (constant T) as explained in Sec. II. As indicated by fine arrows near (0,0) in Fig. 6(b), the modes now, respectively, describe Frenkel pair creation and isothermal recovery by diffusion of both species down the chemical potential gradient.

Within the validity of the model of metals described in Appendix A, the behaviors indicated in Fig. 6 are universal. The modes in Fig. 6(a) pertain to all metals near equilibrium at almost all temperatures, and those in Fig. 6(b) represent all close packed surfaces for temperatures above about $0.4T_m$.

C. Boundary conditions on relaxation modes

The general character of the relaxation modes that solve Eq. (9) is seen above to follow from the relative values of the component terms related to diffusion and to recombination. These lead to modes with limiting behavior either for separate diffusion to sinks of the two species, or to recombination and joint diffusion to sinks. The specific forms of the eigenfunctions and the values of the associated eigenvalues naturally depend, in addition, on the particular boundary conditions that prevail at the sinks. A subtlety connected with these matters, left undefined in Sec. II, is briefly clarified in what follows.

The point to be made is that the boundary conditions must certainly be consistent with the character of the modes they define. In the case of separate diffusion to the sinks by the two defect species, each must satisfy conditions pertinent to that species, and there is no evident requirement that the sink parameters be the same for the two species. Dissimilar interactions with a particular sink may, for example, give that sink an apparently different volume or shape for one species than for the other species. Correspondingly, somewhat different eigenfunctions may be required to describe kinetics for the two species.

This cannot be the case when dominant reactions couple the two species so that their correlated variations are the dominant feature. Eigenfunctions must then be selected that describe *joint* behavior, and this requires that the species satisfy common boundary conditions at the sink. This is important both for recombination modes in which defect densities must change equally in space and time, and also for diffusive modes in which the excess species decay together under a common chemical potential gradient.

IV. SUMMARY

This paper treats reacting antidefects in crystals and on crystal surfaces. It is shown how the relaxation modes of thermal defects near equilibrium depend on a comparison of the rate defects diffuse to sinks with the rate of antidefect reaction. When sinks dominate, the relaxation modes comprise separate diffusion of the two species to sinks. When reactions are dominant, the modes in the long wavelength limit respectively describe recombination and mass flow by both species together to sinks. Using models of standard metal behavior, developed in Appendix A , it is shown that bulk metals near equilibrium remain in the regime of independent diffusion at almost all temperatures, while surface defects on close-packed surfaces are reaction-dominated for temperatures above $\sim 0.4T_m$. A definition is given for the temperature T^* and chemical potential μ^* of the reacting defect assembly. This is employed to monitor the defect assembly during reactions such as those that occur after rapid temperature change. Then T^* and μ^* differ from the lattice temperature T and chemical potential μ, to an extent that measures the propensity of the defect system for energy and particle transfer in such processes as sink nucleation and precipitation. The significance of these concepts for the selection of boundary conditions on relaxation modes is discussed, and the respective relaxation modes of bulk and surface defects identified using the models of bulk metals and close-packed metal surfaces developed in Appendix A. Appendix B introduces universal properties of defect systems that follow for these standard metals.

ACKNOWLEDGMENTS

This work was supported in part by the DOE through the University of Illinois MRL Grant No. DEFG02-91-ER45439. The author thanks Professor M. Ondrejcek and Professor M. Rajappan for helpful discussions.

APPENDIX A: MODELS OF THERMAL DEFECTS FOR STANDARD METALS AND CLOSE-PACKED SURFACES

There is a considerable degree of regularity in the behavior of thermally activated defects in bulk metallic crystals.[2] A comprehensive review is available, with critical selection of data.[12] The regularity is most apparent in the bulk diffusive properties, and extends, remarkably, to crystals of the rare gases, but not to the elemental semiconductors diamond, Si, and Ge, which have low coordination numbers. All the materials with similar properties support dominant vacancy disorder in the bulk, and a resulting vacancy-dominated atomic diffusion. Our purpose here is to collect and correlate the properties of thermal defects, first of the bulk, to model the average behavior as a *standard metal*, and second to carry through a similar assessment for defect properties of its close packed surfaces, to model a *standard close-packed surface*. These prove to be of value in the text by facilitating an assessment of typical regimes of response for defect species in metals.

1. Bulk defects

a. *Bulk vacancy*

The important facts are that diffusion coefficients in metals typically fall within an order of magnitude of 10^{-8} cm^2/s at the melting temperatures, T_m. With activation energies about $17k_BT_m$, and with prefactors within an order of magnitude of 0.3 cm^2/s, the diffusion coefficient approximately obeys

$$\mathrm{D}(T) = 0.3\exp(-17T_m/T)\ \mathrm{cm}^2/\mathrm{s}. \tag{A1}$$

Inspection of documented cases[2,12] reveals that the activation energy typically arises from a vacancy formation energy of $\sim 10k_BT_m$, with an entropy ~ 1 to $2k_B$, so that the vacancy concentration is approximately

$$c_v(T) = 6\exp(-10T_m/T). \tag{A2}$$

A comparison of Eqs. (A1) and (A2) gives the hopping rate as

$$D_v(T) = 5\times 10^{-2}\exp(-7T_m/T)\ \mathrm{cm}^2/\mathrm{s}. \tag{A3}$$

In fact motion energies actually relate more closely to the lattice phonon modes that activate atomic hops, and so the link to cohesion and hence T_m deteriorates for the special case of the alkali metals, which display very low shear moduli.[2,12] Otherwise Eq. (A3) provides a useful estimate of vacancy motion in metals.

b. *Bulk interstitials*

Information about interstitial behavior in metals is less abundant than that for vacancies. Experiment and calculation both reveal that "dumbbell" interstitials are favored, with two atoms occupying a single site symmetrically. The formation energies of interstitials are typically a factor ~ 3 larger than those of vacancies, or $\sim 30k_BT_m$. At the same time, the complexity of the highly distorted lattice near the defect results in many very similar saddlepoints for motion. Related to this same feature is the low activation energy for interstitial migration, typically less than k_BT_m. The activation energy for diffusion by interstitial hopping thus typically remains almost twice that for vacancies, which explains the prevalence of vacancy-facilitated diffusion in metals.

Only recently has it been recognized that the flat energy landscape for interstitial motion has further consequences. One is that interstitials possess resonant vibrational modes,[43] deep in the Debye vibrational tail, whose excitation drives interstitial diffusion. Important here is the phonon entropy $s=\Sigma_i \ln \omega/\omega'$, the sum extending over all modes with, ω', and without, ω, an interstitial. For interstitials s appears to be very large, mainly as a result of the low-frequency resonance modes. Values of $s\sim 16k_B$ are cited from experiments and theory,[36,37,44] and these produce interstitial concentrations larger than otherwise expected by a factor of 10^7. Thus interstitials have

$$c_i \sim 10^7\exp(-30T_m/T). \tag{A4}$$

Still fewer details are known about interstitial motion, other than the easy activation. One useful source of information is computer simulation with interatomic potentials which, while fitted to particular cases, actually are generic, so that the results, when scaled, pertain well to other metals. Such treatments reproduce[37] an interstitial concentration at T_m (for Cu) of just below 10^{-6}, in agreement with Eq. (A4). Interstitial hops appear complex since the activation energy is low and the dwell time accordingly short. From simulations, the interstitial-driven component of diffusion at T_m is close to 10^{-10} cm^2/s. With the small hopping energy the diffusion is only weakly activated, and the resulting interstitial mobility consistent with Eq. (A4) is

$$D_i = 10^{-4}\exp(-0.5T_m/T)\ \mathrm{cm}^2/\mathrm{s}. \tag{A5}$$

The unusually small prefactor may in part be a further consequence of the resonance modes, which result in a small attempt frequency.

The concentrations $\overline{c_1}, \overline{c_2}$ of bulk defects for a standard metal behave as the functions of T_m/T shown as broken lines in Fig. 7. A characterization of the consequences for the reaction kinetics in the equilibrating defect assembly is provided in Sec. II D.

2. Surface defects

Here we turn to the comparative properties of adatoms and advacancies. There is no current demonstration that surface behavior exhibits a regularity comparable with that of the bulk, although the possibility has been introduced.[19] In-

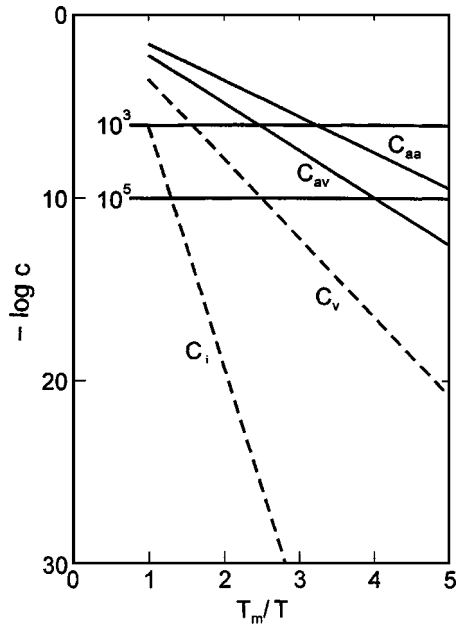

FIG. 7. Concentrations of thermal defects for a standard metal (broken lines) and on close-packed surfaces (solid lines). The notation is (v) vacancy; (i) interstitial; (av) advacancy; and (aa) adatom. The horizontal lines mark the conditions $cN=1$ for sinks separated by $\sim 10^3$ steps and $\sim 10^5$ steps, with N the number of atomic jumps required in the average defect lifetime.

deed, details of atomic mobility on surfaces must evidently depend on the particular orientation of the surface considered. Also, broad studies of equilibrium mass surface diffusion are at present lacking, so there has existed no purpose in seeking trends among metals. Nevertheless, the data currently available for close-packed surfaces differ strikingly from bulk results, to an extent that presents a significant pattern in itself. Specifically, there is a qualitative difference in bulk and surface behavior that is established in a credible manner by the existing (if few) results. This encourages the following characterization of a *standard close-packed surface*.

a. *Adatoms and advacancies*

In several cases surface mass diffusion coefficients on metals have been established by direct experiment.[24,45–47] Reliable prefactors for mass diffusion appear to be $\sim 10^{-4}$–10^{-3} cm^2/s, rather than the bulk value ~ 0.3 cm^2/s. Activation energies for diffusion also are much smaller at $\sim 6k_BT_m$, in place of $17k_BT_m$ for the bulk, giving

$$D \sim 5 \times 10^{-4} \exp(-6T_m/T) \text{ cm}^2/\text{s}. \quad \text{(A6)}$$

Adatoms are thought to be generally the more mobile defect, dominating diffusion on close-packed surfaces in many cases, although accurate information is scarce. The diffusion energy of $\sim 6k_BT_m$ must be apportioned between formation and motion energies. Force model calculations[48–50] show that the adatom formation energy is greatest on the smoothest (close packed) surfaces, as appears reasonable from the surface stability and large surface energies. For such cases as fcc (111) and bcc (011), the hopping energy is perhaps 1 to $2k_BT_m$ and the formation energy 4 to $5k_BT_m$. Detailed experimental studies of hopping confirm for adatoms that the formation portion is generally much larger. These results appear consistent with surface defects on the smoothest surfaces having formation energies in the range $4.5k_BT_m$, and with entropies of ~ 1 to $2k_B$. We thus estimate

$$c \sim 3 \exp(-4.5T_m/T) \quad \text{(A7)}$$

for adatoms; the observed diffusion coefficient (A6) now identifies a hopping mobility

$$D \sim 2 \times 10^{-4} \exp(-1.5T_m/T) \text{ cm}^2/\text{s}. \quad \text{(A8)}$$

Model force Monte Carlo calculations also suggest a systematic variation of hopping energy with host properties (parametrized by a Lennard–Jones potential), with much the same magnitude as in Eq. (A8).[48]

Here two points warrant specific comment. It is interesting first that the adatom on smooth surfaces and the bulk interstitial both have small prefactors $\sim 10^{-4}$ cm^2/s to match their small activation energies for hopping. This may derive in part from the low frequencies of phonon modes that drive the process, as mentioned above. It seems possible for adatoms that the formation entropy could in fact be larger for this same reason, and the migration prefactor correspondingly smaller still. Careful measurements for more strongly bound surface species with larger activation energies generally give larger prefactors than 10^{-3} cm^2/s, as again appears reasonable.[32] Second, adatom formation energies are believed to be generally still smaller on less smooth crystal faces, so that the large defect populations near T_m given in Sec. III of the text using Eq. (A6) probably underestimate the actual defect densities for surfaces other than the smoothest.

As it is poorly established which surface species dominates diffusion in most cases, there is correspondingly little information available about the contributions of minority species, perhaps often advacancies. Pair bond models predict identical formation energies for the two surface species and are typically incorrect by a factor of 3 or more in absolute energy, owing to relaxation near the surface. Entropic factors certainly favor adatoms with low-frequency modes in the surface plane. Given that advacancies are the minority species, reasonable guesses for vacancylike behavior on smooth surfaces are

$$c \sim 3 \exp(-6T_m/T); \quad \text{(A9)}$$

$$D \sim 3 \times 10^{-4} \exp(-2T_m/T) \text{ cm}^2/\text{s}. \quad \text{(A10)}$$

The characteristics of a standard close-packed surface (SCPS) as assessed here present a picture strikingly different from that for bulk defects. The solid lines in Fig. 7 show concentrations of surface defects that are much larger than those of bulk defects, and remain as large as $\sim 10^{-6}$ down to temperatures as low as $T_m/3$.

The meaning this difference lends to defect reactions is clarified by consideration of the typical life cycle when sinks are $\sim 10^3$ atom-spacings distant. Examples are films ~ 0.2 μm thick, for which the surfaces act as the sinks for bulk defects, or when a crystal surface is miscut by $\sim 0.1°$ to

give a similar spacing of surface steps, which act as sinks for surface defects. Then, in each example, $N \sim 10^6$ steps are needed in a typical random walk of a defect lifespan from sink to sink. Since $cN > 1$ at all temperatures above $T_m/3$, Fig. 7 shows that a surface defect will normally encounter its antidefect and annihilate long before the walk is complete. Therefore reactions on terraces provide the dominant process of annihilation in the defect life cycle. It follows from detailed balance that creation of defect pairs spontaneously from fluctuations on the terraces must, under the same conditions, correspondingly be the dominant mechanism by which thermal defects also form, together with a small fraction created singly at the sinks. This conclusion may hold down to still lower reduced temperatures for *non*-close-packed surfaces, owing to the larger densities of thermal defects they support (see above).

These distinctions concerning the defect life cycle point to the need for treatments of defect flow that describe interacting defect assemblies, particularly for surface-related phenomena. The extension to circumstances where external driving processes, such as irradiation, cause the system, either bulk or surface, to develop excess defect populations, also is deferred to a later work.[11]

In equilibration, the product of the two thermal equilibrium concentrations is an important quantity. For the standard metal defined above these are

$$\text{Bulk: } \overline{c_1}\overline{c_2} = 6 \times 10^7 \exp(-40T_m/T); \qquad \text{Surface: } \overline{c_1}\overline{c_2} = 9 \exp(-10.5T_m/T). \tag{A11}$$

One further point, pertaining to the bulk and surface formation energies estimated above, is that both bulk vacancies and bulk interstitials bind strongly to ordinary surface sites to form advacancies and adatoms on the surface terraces in the two cases. By subtracting the surface formation free energies from the bulk values one finds that the binding free energies to the surface are $\sim k_B(4T_m - T)$ and $\sim k_B(25T_m - 15T)$ for vacancies and interstitials, respectively. These are the free energy differences that must be accommodated in the detailed balance of the transition rates between bulk and surface defect species.

APPENDIX B: UNIVERSAL BEHAVIOR IN THE RESPONSE OF THE STANDARD METAL

Both the kinetics and the equilibrium configurations of the standard models outlined above depend only on T/T_m. This leads to remarkable predictions of behavior that are universal for all metals at the homologous temperatures, merely scaled from the actual temperature by T_m. As an example, the quenching characteristics discussed in Sec. III A fall in this category. In particular, different metals are expected to evolve along similar paths given the same fractional quenches. Furthermore, since the model kinetics are defined by similarly homologous behavior, with fixed prefactors, and activation energies that scale with T_m, the time evolutions of different systems under homologous conditions are predicted to exhibit *identical* response times, as in Fig. 5. In what follows, several further relationships in diverse contexts are identified.

1. Epitaxial growth

In the growth of single crystal films by molecular beam epitaxy, it is desirable to have the diffusion of surface atoms fast enough for added atoms to reach steps, say 10 nm distant, during deposition of a monolayer, requiring perhaps 10 s. At the same time bulk diffusion must be sufficiently slow that mixing through one monolayer of penetration requires more than the net growth time of perhaps 10^4 s. We solve Eq. (A5) for T given the required surface diffusion to find $T > 0.28T_m$, this would be higher on rougher surfaces). Upon solving Eq. (A3) for the necessary bulk diffusion we find $T < 0.39T_m$. Evidently the necessary growth conditions occur for $T \sim 0.33T_m$. This result is consistent with an experimental determination[51,19] that optimal growth for normal metallic crystals occurs for $T \sim 3T_m/8$.

2. Competition between bulk and surface diffusion in surface processes

The flow of atoms required to smooth surface scratches or to support fluctuations of step edge profile may be supplied by diffusion of defects across terraces or by diffusion of defects through the bulk. The larger activation energy of the bulk process opens the possibility that a crossover occurs from a surface dominated process at low temperature to a bulk-dominated process at high temperature. In the case of step edges the effective diffusion coefficient is[46]

$$D \sim D_b + qaD_s, \tag{B1}$$

with q the wave vector of the fluctuation along the step, a the atomic spacing along the step, and subscripts b and s identifying bulk and surface mass diffusion coefficients. For fluctuations of wavelength 1 μm, so that $qa \sim 10^{-3}$, the bulk and surface diffusion coefficients given in Appendix A now yield equal contributions when $10^{-8} \exp(-11T_m/T) = 1$, or $T \approx 0.6T_m$. Experiments for fluctuations of this wavelength using low energy electron microscopy have identified the crossover from surface- to bulk-driven fluctuations for Pt (111) precisely in this predicted temperature range.[46] For surface scratches the q dependence differs but the crossover again occurs as predicted.[24,25] Similar crossovers are predicted for all metals in the same temperature range, for both step fluctuations and scratch annealing, on all close-packed surfaces, according to the standard model described here.

3. Radiation-enhanced bulk diffusion

An irradiation flux creates Frenkel pairs in the bulk, and the additional defects so created enhance the diffusion of atoms through the bulk. The diffusion in all unirradiated metal is vacancy dominated, and it turns out, since irradiation-induced interstitials precipitate, that diffusion is enhanced by the ratio of the total to the equilibrium vacancy concentration. For a film of thickness L, vacancies drain to the surfaces with time constant $\tau^{-1} = q^2 D_v$, with $q = \pi/L$, so

that a creation rate K per site causes a steady state excess occupation $c=K/q^2D_v$. Thus the coefficient of mass diffusion required to double the vacancy concentration is $D=K/q^2$, and, from Eq. (A1), the temperature at which the irradiation field K doubles the vacancy concentration is

$$T \approx -17T_m/\ln(KL^2/3). \tag{B2}$$

This result is, once more, universal. Taking the temperature T_m as an example, all thin films of pure metal 1 μm thick require $K \sim 12\ s^{-1}$ in order to double the vacancy concentration, the excess being greater at lower $T<T_m$. Similarly, for a 0.3 μm film with $K=1.5\times10^{-5}\ s^{-1}$ (the experimental maximum that avoids blistering) Eq. (B2) predicts that the vacancy concentration (and hence the mass diffusion coefficient also) is doubled at $T\sim0.53T_m$. For Cu_3Au, Lee *et al.*[33] find that the experimental value is $\sim0.58T_m$, in reasonable accord with the universal prediction.

4. Beam-assisted growth

It may be appropriate to terminate these speculative comments with a prediction. Suppose that a beam of self-ions were employed to speed up surface kinetics; what conditions would be needed to promote measurable results—say a doubling of surface defect density and hence diffusion also? We use a beam energy that creates one defect pair per incident particle, and a readily achievable ion beam current of $1\ \mu A\ cm^{-2}(\sim10^{13}\ cm^{-2}\ s^{-1}$ or $K=10^{-2}\ s^{-1})$, for a crystal with surface miscut by 0.1°, so that the surface sinks are steps spaced by $L=100$ nm. The required condition $K\sim q^2D=(\pi/L)^2D$ is achieved for a surface mass diffusion coefficient $D=10^{-13}\ cm^2/s$, which from Eq. (A6) requires $T\sim0.3T_m$. Evidently a somewhat larger flux density than $1\ \mu A/cm^2$ may be required to accelerate kinetics significantly at the slightly higher temperature $\sim3T_m/8$ at which single crystal films of metals are often grown epitaxially.

[1] Y. Adda and J. Phillibert, *La Diffusion dans les Solides* (Universitaires de France, Paris, 1966).
[2] C. P. Flynn, *Point Defects and Diffusion* (Oxford University, New York, 1972).
[3] P. G. Shewman, *Diffusion in Solids* (McGraw-Hill, New York, 1963).
[4] A. B. Lidiard, *Handbuch der Physik 20* (Springer-Verlag, Berlin, 1957).
[5] M. E. Glicksman, *Diffusion in Solids* (Wiley, New York, 2000).
[6] A. Pimpinelli and J. Villain, *Physics of Crystal Growth* (Cambridge University Press, Cambridge, U.K., 1998).
[7] A. Zangwill, *Physics at Surfaces* (Cambridge University Press, Cambridge, U.K., 1988).
[8] A. G. Naumovets and Z. Zhang, Surf. Sci. **500**, 414 (2002).
[9] G. J. Dienes and G. H. Vineyard, *Radiation Effects in Solids* (Interscience, New York, 1957).
[10] R. S. Averback and T. Diaz de la Rubia, *Solid State Physics 51*, edited by H. Ehrenreich and F. Spaepen (Academic, New York, 1997).
[11] C. P. Flynn (to be published).
[12] P. Ehrhart, *Landolt-Bornste in New Series, Group III*, Vol. 25, edited by H. Ullmaier (Springer, Berlin, 1991), p. 115.
[13] R. Gomer, Rep. Prog. Phys. **53**, 917 (1990).
[14] A. G. Naumovets and Y. S. Vedula, Surf. Sci. Rep. **4**, 365 (1985).
[15] G. L. Kellogg, Surf. Sci. Rep. **21**, 1 (1994).
[16] T. Ala-Nissila, R. Ferrando and S. C. Ying, Adv. Phys. **51**, 949 (2002).
[17] D. Lazarus, *Solid State Physics 10*, edited by F. Seitz and D. Turnbull (Academic, New York, 1962).
[18] J. Van Liempt, Z. Phys. **96**, 534 (1935).
[19] C. P. Flynn, J. Phys. F: Met. Phys. **18**, L195 (1988).
[20] N. C. Bartelt, J. L. Goldberg, T. L. Einstein, and E. D. Williams, Surf. Sci. **273**, 252 (1992).
[21] H.-C. Jeong and E. D. Williams, Surf. Sci. Rep. **34**, 171 (1999).
[22] P. Nozières, in *Solids Far From Equilibrium*, edited by C. Godrèche (Cambridge University Press, Cambridge, U.K., 1991), p. 1.
[23] C. P. Flynn, Phys. Rev. B **66**, 155405 (2002).
[24] J. M. Blakely and H. Mykura, Acta Metall. **10**, 565 (1962).
[25] W. W. Mullins, J. Appl. Phys. **30**, 77 (1959).
[26] J. Frenkel, Z. Phys. **35**, 652 (1926); W. Schottky, Z. Phys. Chem. Abt. B **29**, 335 (1935); see e.g., Ref 4.
[27] M. deJong and J. S. Koehler, Phys. Rev. **131**, 49 (1963).
[28] C. P. Flynn, Phys. Rev. **134**, A241 (1964).
[29] T. E. Volin and R. W. Balluffi, Phys. Status Solidi **25**, 163 (1968).
[30] R. E. Hoffman, D. Turnbull, and F. E. Hart, Acta Metall. **3**, 417 (1955); R. E. Hoffman, *ibid.* **6**, 95 (1958).
[31] Quenching methods actually measure c_1-c_2, cf. R. M. Tromp and M. Mankos, Phys. Rev. Lett. **81**, 1050 (1998).
[32] See, for example, S. C. Wang and G. Ehrlich, Surf. Sci. **206**, 451 (1988), and the review in Ref. 10.
[33] Y. S. Lee, C. P. Flynn, and R. S. Averback, Phys. Rev. B **60**, 881 (1999).
[34] A. D. Brailsford and R. Bullough, Philos. Trans. R. Soc. London, Ser. A **302**, 87 (1981).
[35] N. V. Doan and G. Martin, Phys. Rev. B **67**, 134107 (2003). There, the term in $\overline{c_1}\overline{c_2}$ is omitted or perhaps included in K_1, K_2. It is, however, essential for the linear theory.
[36] A. V. Granato, Phys. Rev. Lett. **68**, 974 (1992).
[37] K. Nordlund and R. S. Averback, Phys. Rev. Lett. **80**, 4201 (1998).
[38] See, for example, S. Hoshimo, Proc. Phys. Soc. Jpn. **12**, 315 (1957).
[39] J. W. M. Frenken, B. J. Hinch, J. P. Toennies, and C. Woll, Phys. Rev. B **41**, 938 (1990); J. F. van der Veen, B. Pais, and A. W. Denier van der Gon, in *Kinetics of Ordering and Growth on Surfaces*, edited by M. Lagally (Plenum, New York, 1990).
[40] S. C. Wang, U. Kurpick, and G. Ehrlich, Phys. Rev. Lett. **81**, 4923 (1998); S. C. Wang and G. Ehrlich, *ibid.* **79**, 4234 (1997); and for earlier work, R. Fink, in *Diffusion at Interfaces-Microscopic Concepts*, edited by M. Grunze, H. J. Kreuzer, and J. J. Weimer (Springer-Verlag, Berlin, 1988).
[41] G. Martin and P. Bellon, *Solid State Physics 50*, edited by H. Ehrenriech and F. Spaepen (Academic, New York, 1996).

[42] A. C. Lund and C. A. Schuh, Phys. Rev. Lett. **91**, 235505 (2003).
[43] See P. H. Dederichs and R. Zeller, *Point Defects in Materials II: Springer Tracts on Modern Physics 87* (Springer, Berlin, 1980).
[44] C. A. Gordon, A. V. Granato, and R. O. Simmons, J. Non-Cryst. Solids **205**, 216 (1996).
[45] D. W. Bassett, in *Surface Mobilities on Solid Materials*, edited by V. T. Bihn (Plenum, New York, 1983).
[46] M. Ondrejcek, W. Swiech, G. Yang, and C. P. Flynn, Philos. Mag. Lett. **84**, 69 (2004).
[47] M. Ondrejcek, M. Rajappan, W. Swiech, and C. P. Flynn, J. Phys.: Condens. Matter (to be published).
[48] P. M. Agrawal, B. M. Rice, and D. L. Thompson, Surf. Sci. **515**, 21 (2002).
[49] Y. N. Devyatko, S. V. Rogozhkin, and A. V. Fadeev, Phys. Rev. B **63**, 193401 (2001).
[50] S. V. Eremeev, A. G. Lipnitskii, A. I. Potekeev, and E. V. Chulkov, Phys. Low-Dimens. Semicond. Struct. **3–4**, 127 (1997).
[51] J. E. Cunningham and C. P. Flynn, J. Phys. F: Met. Phys. **15**, L221 (1985).